

# Non-invasive imaging of drug-induced liver injury with $^{18}\text{F}$ -DFA PET

Jessica R. Salas<sup>1,2</sup>, Bao Ying Chen<sup>1,2</sup>, Alicia Wong<sup>1,2</sup>, Sergio Duarte<sup>3</sup>, Stephanie A. K. Angarita<sup>3</sup>,  
Gerald S. Lipshutz<sup>1,4,5</sup>, Owen N. Witte<sup>1,4,6</sup>, Peter M. Clark<sup>1,2,4,‡</sup>

<sup>1</sup> Department of Molecular and Medical Pharmacology, <sup>2</sup> Crump Institute for Molecular Imaging, <sup>3</sup> Department of Surgery, <sup>4</sup> Eli and Edythe Broad Center of Regenerative Medicine and Stem Cell Research, <sup>5</sup> Intellectual and Developmental Disabilities Research Center, <sup>6</sup> Department of Microbiology, Immunology and Molecular Genetics, University of California, Los Angeles CA 90095.

‡ Correspondence should be addressed to Peter M. Clark, Crump Institute, Box 951770, 4333 CNSI, Los Angeles, CA 90095-1770; 310-267-4755; [pclark@mednet.ucla.edu](mailto:pclark@mednet.ucla.edu)

First author: Jessica R. Salas, Crump Institute, Box 951770, 4333 CNSI, Los Angeles, CA 90095-1770; 310-267-4755; [cunninj20@k-state.edu](mailto:cunninj20@k-state.edu) (Researcher)

*Word count: 5,000*

*Financial support:* Financial support for this work was provided by the NIH, the Parker Institute for Cancer Immunotherapy, and the Broad Stem Cell Research Center at UCLA. PMC and ONW are inventors on a patent, held by the Regents of the University of California, that describes the  $^{18}\text{F}$ -DFA radiotracer.

*Running title:* Imaging liver injury with  $^{18}\text{F}$ -DFA PET

*Key words:* PET imaging, drug-induced liver failure, hepatocytes

## Abstract

Drug-induced liver failure is a significant indication for a liver transplant, and unexpected liver toxicity is a major reason that otherwise effective therapies are removed from the market. Various methods exist for monitoring liver injury but are often inadequate to predict liver failure. New diagnostic tools are needed. **Methods.** We evaluate in a preclinical model whether  $^{18}\text{F}$ -2-deoxy-2-fluoroarabinose ( $^{18}\text{F}$ -DFA), a PET radiotracer that measures the ribose salvage pathway, can be used to monitor acetaminophen-induced liver injury and failure. Mice treated with vehicle, 100, 300, or 500 mg/kg acetaminophen for 7 or 21 hours were imaged with  $^{18}\text{F}$ -FDG and  $^{18}\text{F}$ -DFA PET. Hepatic radiotracer accumulation was correlated to survival and percent of non-necrotic tissue in the liver. Mice treated with acetaminophen and vehicle or *N*-acetylcysteine were imaged with  $^{18}\text{F}$ -DFA PET.  $^{18}\text{F}$ -DFA accumulation was evaluated in human hepatocytes engrafted into the mouse liver. **Results.** We show that hepatic  $^{18}\text{F}$ -DFA accumulation is 49 - 52% lower in mice treated with high dose acetaminophen than in mice treated with low or no dose acetaminophen. Under these same conditions, hepatic  $^{18}\text{F}$ -FDG accumulation was unaffected. At 21 hours post-acetaminophen treatment, hepatic  $^{18}\text{F}$ -DFA accumulation can distinguish mice that will succumb to the liver injury from those that will survive it (6.2 versus 9.7 signal/background, respectively). Hepatic  $^{18}\text{F}$ -DFA accumulation in this model provides a tomographic representation of hepatocyte density in the liver, with a  $R^2$  between hepatic  $^{18}\text{F}$ -DFA accumulation and percent non-necrotic tissue of 0.70. PET imaging with  $^{18}\text{F}$ -DFA can be used to distinguish effective from ineffective resolution of acetaminophen-induced liver injury with *N*-acetylcysteine (15.6 versus 6.2 signal/background, respectively). Human hepatocytes, in culture or engrafted into a mouse liver, have similar levels of ribose salvage activity to mouse hepatocytes. **Conclusions.** Our findings suggest that PET imaging with  $^{18}\text{F}$ -DFA can be used to visualize and quantify drug-induced acute liver injury and may provide information on the progression from liver injury to hepatic failure.

## Introduction

Drug-induced liver injury can be provoked by a variety of agents including tyrosine kinase inhibitors (Pazopanib), antibody-drug conjugates (Trastuzumab emtansine), and analgesics (acetaminophen) (1–3), is a frequent indication for a liver transplant, and is a major reason for post-market drug warnings and withdrawal (4–6). Various methods exist for assessing liver health during drug-induced liver injury. These include static measurements of liver-selective enzymes and metabolites, such aspartate transaminase (AST), alanine transaminase (ALT), and bilirubin; liver biopsies; and imaging with computed tomography (CT), magnetic resonance imaging, and ultrasound (1,4,5,7–12). All of these methods have proven clinical value but do not provide a complete picture of liver health. In particular, specifically identifying patients who will progress from acute liver injury to fulminant liver failure remains a clinical challenge (1,6,13,14). Tomographic molecular imaging of select liver functions could provide additional information not captured with these other methods.

Recently we developed two PET tracers,  $^{18}\text{F}$ -2-deoxy-2-fluoroarabinose ( $^{18}\text{F}$ -DFA) and  $^{18}\text{F}$ -2-deoxy-2-fluororibose ( $^{18}\text{F}$ -2-DFR), to measure ribose salvage activity (15,16). The ribose salvage pathway is most active in the liver, leading to significant and specific accumulation of  $^{18}\text{F}$ -DFA,  $^{18}\text{F}$ -2-DFR, and their metabolites in this organ (15,16). Previously we showed that hepatic  $^{18}\text{F}$ -DFA and  $^{18}\text{F}$ -2-DFR accumulation are lower in mouse models of fatty liver disease and, in a limited study, in mice treated with one dose of acetaminophen (300 mg/kg) at one specific time point (24 hours post-injection) (15,16). However various questions remain on a potential role for  $^{18}\text{F}$ -DFA in imaging liver injury and failure.

We hypothesized that  $^{18}\text{F}$ -DFA PET imaging could be used to non-invasively monitor and study acetaminophen-induced liver injury and failure. Though we previously showed that  $^{18}\text{F}$ -2-DFR was subject to less defluorination than  $^{18}\text{F}$ -DFA (16),  $^{18}\text{F}$ -DFA was chosen to be studied here due to the commercial availability of the synthetic precursor and the fact that  $^{18}\text{F}$ -DFA could be

prepared on an automated radiosynthesizer (17). Our results suggest that PET imaging with a radiotracer that measures ribose salvage activity can be used to monitor acute liver failure and may provide information not available with current diagnostic methods.

## **Materials and Methods**

*Mice:* C57Bl/6 male mice (10 – 11 weeks old) were used for all experiments unless otherwise noted. All animal experiments were approved by the UCLA Animal Research Committee.

*Drug treatments:* Acetaminophen: Mice, fasted overnight, were injected intraperitoneal with vehicle or acetaminophen (15 mg/mL in 0.9% w/v saline). N-acetylcysteine (NAC): Mice were injected intraperitoneal with vehicle or NAC (1200 mg/kg), 1 or 4 h after acetaminophen treatments.

*Serum AST, ALT, and bilirubin levels:* ALT and AST Liquid Reagent Set (Pointe Scientific) and Bilirubin Assay (Sigma-Aldrich) kits were used following the manufacturer's protocol except that all the reagents and samples were scaled down 10-fold.

*Histological analyses:* The right liver lobe was removed, washed in 1X PBS, and fixed (10% formalin, 1 d). Sections were stained for H&E or with an antibody against FAH (Yecuris 20-0034; 1:1000; RT, 1 h). Percent of FAH expressing hepatocytes and non-necrotic tissue was quantified with Ilastik (Version 1.2.0) and ImageJ (Version 1.51n) (18,19).

*PET tracers:*  $^{18}\text{F}$ -DFA was synthesized as described (17).  $^{18}\text{F}$ -FDG was obtained from the UCLA Translational Imaging Division.

*PET/CT imaging:* Mice were injected with ExiTron nano 12000 (100  $\mu\text{L}$ ), 3 days before the PET imaging experiment. Mice were anesthetized, injected with  $\sim 2.96$  MBq of  $^{18}\text{F}$ -FDG (after an overnight fast) or  $^{18}\text{F}$ -DFA, and after 60 minutes, imaged for 10 minutes on a G8 PET/CT (SOFIE

Biosciences). Different cohorts of mice were used for the 7 and 21 hour post-acetaminophen treatment  $^{18}\text{F}$ -DFA imaging experiments.

*PET quantification:* An observer unaware of the treatment groups performed the PET quantification using only the CT image to place the regions of interest.  $^{18}\text{F}$ -DFA and  $^{18}\text{F}$ -FDG accumulation are normalized to their respective accumulation in the brain and right forelimb triceps. Brain was used as a reference region for the quantification of  $^{18}\text{F}$ -DFA accumulation as we have never identified specific accumulation of  $^{18}\text{F}$ -DFA in the brain and the same brain region could be readily identified and quantified across different mice. Image-derived blood  $^{18}\text{F}$ -DFA levels were quantified from the left ventricle. Hepatic  $^{18}\text{F}$ -DFA contrast, correlation, and entropy were determined using the GLCM Texture plugin in ImageJ (Version 1.50i) (19).

*Autoradiography:* Autoradiography was performed as described (20).

*$^3\text{H}$ -ribose accumulation:* Mouse hepatocytes were isolated as described (15). Human hepatocytes (Corning Inc; Lot #373) were plated following the manufacturer's protocol.  $^3\text{H}$ -ribose accumulation experiments were performed as described (15).

*Statistics:* Data is plotted as mean  $\pm$  standard error of the mean (SEM). Experiment-specific statistical tests are described in their respective figure legends. All analyses were performed using GraphPad Prism (Version 7.01).

*Detailed procedures describing the FRG mouse model of acute liver failure, human hepatocyte engraftment into FRG mice, and mouse experiment numbers can be found in the Supplemental Methods.*

## **Results**

*A mouse model of drug-induced liver injury.* Mice provide a model system in which to study drug-induced liver injury (21–23). Consistent with published results, we found that mice succumb to acetaminophen-induced liver injury in a dose dependent manner. All of the mice treated with 100 mg/kg acetaminophen survived, but only ~50% and ~10% of the mice treated with 300 mg/kg and 500 mg/kg acetaminophen, respectively, survived (**Fig. S1A**). The earliest time point at which maximum ALT levels occur in mice is 7 hours post-acetaminophen treatment (24,25), and mice treated with 500 mg/kg acetaminophen succumb to liver failure starting at 24 hours post-treatment (**Fig. S1A**). Therefore, we chose to study mice at 7 and 21 hours post-acetaminophen treatment. Mice treated with high dose (300 and 500 mg/kg) acetaminophen for 7 and 21 hours had elevated serum ALT and AST levels, and liver sections from these mice displayed significant necrosis in Zone 3 hepatocytes by H&E staining (**Fig. S1B – D**). These studies validate our mouse model and provide us with a system in which to test our hypothesis.

*PET imaging with <sup>18</sup>F-FDG cannot distinguish vehicle-treated from high dose (500 mg/kg) acetaminophen-treated mice.* <sup>18</sup>F-FDG is the most widely used PET tracer although its potential utility in studying liver disease is complicated by the hormonal regulation of liver glucose consumption (26–28). We first tested the utility of <sup>18</sup>F-FDG imaging for studying drug-induced liver injury. Serum AST and ALT levels were elevated but hepatic <sup>18</sup>F-FDG accumulation was unaffected ( $p=0.56$ ) in mice 7 and 21 hours after treatment with 500 mg/kg acetaminophen (**Fig. S2A – C**). This suggests that PET imaging with <sup>18</sup>F-FDG will be unable to provide information on acetaminophen induced liver injury.

*PET imaging with <sup>18</sup>F-DFA 7 hours after acetaminophen treatment can distinguish low (100 mg/kg) and high (300 and 500 mg/kg) dose acetaminophen-treated mice but cannot distinguish*

mice that will survive high dose (300 and 500 mg/kg) acetaminophen from those that will not. The radiotracer  $^{18}\text{F}$ -DFA accumulates strongly in liver hepatocytes through ribose salvage activity (15), and its accumulation could be affected by acetaminophen. High dose (300 and 500 mg/kg) acetaminophen treatment caused a significant 52% decrease in hepatic  $^{18}\text{F}$ -DFA accumulation compared to low dose (100 mg/kg) acetaminophen and vehicle treatment ( $p < 0.0001$ ; **Fig. 1A, B**).  $^{18}\text{F}$ -DFA accumulation in the mice treated with high dose (300 and 500 mg/kg) acetaminophen was significantly higher in the kidneys and intestines ( $p = 0.0007$  and  $p = 0.001$ , respectively) but similar in other organs including the lungs and heart compared to vehicle-treated mice (**Fig. S3A**), potentially suggesting increased renal excretion and intestinal accumulation of the radiotracer in the absence of specific hepatic accumulation. These results were independent of whether organ-specific  $^{18}\text{F}$ -DFA accumulation was normalized to brain  $^{18}\text{F}$ -DFA accumulation or image-derived blood  $^{18}\text{F}$ -DFA levels (**Fig. S3B**). The decrease in hepatic  $^{18}\text{F}$ -DFA accumulation was similar in mice treated with either 300 or 500 mg/kg acetaminophen ( $p = 0.05$ ) and was indistinguishable between the high dose (300 and 500 mg/kg) acetaminophen-treated mice that would survive the injury and those that would not ( $p = 0.50$ ; **Fig. 1A, C**). As expected (1), ALT, AST, and total bilirubin levels also failed to discriminate between mice that survived high dose (300 and 500 mg/kg) acetaminophen from those that did not ( $p = 0.56$ ,  $p = 0.70$ ,  $p = 0.98$ , respectively; **Fig. 1D**). Visually all the mice looked equally sick.

These results could be broadly applicable across various types of acute liver injury or could be specific to acetaminophen toxicity. Immunodeficient mice lacking the enzyme fumarylacetoacetate hydrolase (*Fah*<sup>-/-</sup>/*Rag2*<sup>-/-</sup>/*Ii2rg*<sup>-/-</sup> or FRG mice) undergo liver failure in the absence of the drug 2-(2-nitro-4-trifluoromethylbenzoyl)-1,3-cyclohexanedione (NTBC) following buildup of the hepatotoxic tyrosine catabolite fumarylacetoacetate (29). FRG mice withdrawn from NTBC for 2 weeks displayed histological evidence of hepatocyte damage compared to mice maintained on NTBC and succumb to liver failure within ~2.5 weeks (**Fig. S4A, B**). The amount

of hepatocellular damage in this model is considerably less than in the acetaminophen model. Hepatic  $^{18}\text{F}$ -DFA accumulation was 23% lower in FRG mice withdrawn from the NTBC for 2 weeks compared to hepatic  $^{18}\text{F}$ -DFA accumulation in these mice immediately before withdrawing the NTBC ( $p=0.007$ ; **Fig. S4C, D**), suggesting that  $^{18}\text{F}$ -DFA PET could image liver injury and failure caused by multiple different sources.

*PET imaging with  $^{18}\text{F}$ -DFA 21 hours after acetaminophen treatment can distinguish mice that will survive high dose (300 and 500 mg/kg) acetaminophen from mice that will not.* At 21 hours post-acetaminophen treatment, mice treated with high dose (300 and 500 mg/kg) acetaminophen had 49% lower hepatic  $^{18}\text{F}$ -DFA accumulation than mice treated with vehicle and 100 mg/kg acetaminophen ( $p<0.0001$ ; **Fig. 2A, B**). Unlike the 7 hours post-acetaminophen treatment results, hepatic  $^{18}\text{F}$ -DFA accumulation could clearly distinguish mice that would survive the high dose (300 and 500 mg/kg) acetaminophen treatment from those that would not ( $p=0.0003$ ; **Fig. 2A, C**). Hepatic  $^{18}\text{F}$ -DFA accumulation in mice treated with high dose (300 and 500 mg/kg) acetaminophen that survive was intermediate between  $^{18}\text{F}$ -DFA accumulation in non-surviving mice and in vehicle-treated mice (**Fig. 2B, C**). ALT, AST, and total bilirubin levels could not distinguish mice that survived the high dose (300 and 500 mg/kg) acetaminophen treatment from those that did not ( $p=0.26$ ,  $p=0.59$ ,  $p=0.73$ , respectively; **Fig. 2D**), and all the mice looked equally sick.

PET images contain voxel level values from which textural features, such as entropy, contrast, and variability, can be extracted (30–32). These additional features can be better predictors of radiochemotherapeutic responses in esophageal and non-small cell lung cancers and may suffer less variability than bulk values such as mean tracer accumulation (30,31). Voxel-to-voxel hepatic correlation in  $^{18}\text{F}$ -DFA accumulation was higher, and voxel-to-voxel hepatic contrast and entropy in  $^{18}\text{F}$ -DFA accumulation were lower in the mice that did not survive the high

dose (300 and 500 mg/kg) acetaminophen treatment compared to the mice that did ( $p=0.002$ ,  $p=0.0004$ ,  $p=0.0006$ , respectively; **Fig. S5A – C**). This is consistent with an overall decrease in voxels with high  $^{18}\text{F}$ -DFA accumulation across the liver in the non-surviving cohort of mice but also suggests that the distribution of healthy hepatic tissue across the liver may be important for determining the physiological effects of high dose (300 and 500 mg/kg) acetaminophen. Notably the coefficient of variation for the entropy measurements is lowest among all the measured values, suggesting that it may serve as the best quantity for studying drug-induced liver injury.

Combining the results from both time points provides a kinetic picture of the liver responding to high dose (300 and 500 mg/kg) acetaminophen in surviving and non-surviving cohorts (**Fig. S6**). Consistent with immunohistochemical and serum analyses, the data indicate that all mice, independent of survival, suffer significant and possibly equivalent liver damage within 7 hours of high dose (300 and 500 mg/kg) acetaminophen treatment. Only mice that begin to recover hepatic  $^{18}\text{F}$ -DFA accumulation within 21 hours of the acetaminophen treatment will survive. Mice whose hepatic  $^{18}\text{F}$ -DFA accumulation is unchanged from 7 to 21 hours do not survive.

*$^{18}\text{F}$ -DFA PET provides a tomographic representation of hepatocyte density in the liver during acetaminophen-induced liver injury.* The livers of mice treated with high dose (300 and 500 mg/kg) acetaminophen undergo considerable necrosis (**Fig. S1D**).  $^{18}\text{F}$ -DFA accumulation could correlate with the amount of non-necrotic liver tissue. Digital autoradiography of liver sections of mice treated with 300 mg/kg acetaminophen and injected with  $^{18}\text{F}$ -DFA displayed heterogeneous  $^{18}\text{F}$ -DFA accumulation compared to liver sections of vehicle-treated mice (**Fig. 3A**), consistent with the heterogeneous pattern of necrosis present in liver sections of 300 mg/kg acetaminophen-treated mice (**Fig. S1D**). The percent of non-necrotic liver tissue from mice treated with 300 mg/kg acetaminophen significantly correlated ( $R^2 = 0.70$ ;  $p$  value for slope being significantly non-zero:

0.018) with hepatic  $^{18}\text{F}$ -DFA accumulation in the same mice (**Fig. 3B**). Collectively the data suggest that in this system, hepatic  $^{18}\text{F}$ -DFA accumulation as measured by PET imaging provides a whole organ view of functional hepatocyte density in the liver.

*PET imaging with  $^{18}\text{F}$ -DFA can monitor the efficacy of treatments for acetaminophen overdose.*

In other fields, PET imaging has proven effective for monitoring therapeutic responses (33). Approved therapies for acetaminophen overdose are limited but new treatments are in development (34,35).  $^{18}\text{F}$ -DFA PET imaging could potentially monitor the efficacy of these treatments and provide data to complement or anticipate changes in blood biochemistry measurements. NAC administration at different time points post-acetaminophen treatment provides a useful model in which to determine whether PET imaging with  $^{18}\text{F}$ -DFA can distinguish mice that have or have not been successfully treated for acetaminophen toxicity. Consistent with published results (36), acetaminophen-induced hepatic necrosis was blocked by NAC treatment 1 but not 4 hours after 300 mg/kg acetaminophen treatment (**Fig. 4A**). Mice treated with 300 mg/kg acetaminophen followed by NAC 1 hour later accumulated  $^{18}\text{F}$ -DFA in the liver at levels similar to vehicle-treated mice ( $p=0.88$ ) and significantly higher than mice treated with NAC 4 hours after 300 mg/kg acetaminophen treatment ( $p=0.009$ ; **Fig. 4B, C**). Hepatic  $^{18}\text{F}$ -DFA accumulation in mice treated with 300 mg/kg acetaminophen followed by NAC 4 hours later was indistinguishable from hepatic  $^{18}\text{F}$ -DFA accumulation in mice treated only with 300 mg/kg acetaminophen ( $p=0.09$ ; **Fig. 2B, 4C**). These results suggest that  $^{18}\text{F}$ -DFA PET imaging can function as a biomarker to monitor therapies to treat acute liver injury.

*Ribose salvage activity is similar between mouse and human hepatocytes.*  $^{18}\text{F}$ -DFA is not yet approved for use in humans, but isolated human hepatocytes can be analyzed in culture and

engrafted into mice.  $^{18}\text{F}$ -DFA measures ribose salvage activity (15). Isolated mouse and human hepatocytes in culture consume ribose at a similar rate ( $p=0.31$ ; **Fig. 5A**).

Human hepatocytes administered to FRG mice can engraft into and repopulate the liver of these mice following NTBC withdrawal (29). FRG mice were engrafted with human hepatocytes and imaged with  $^{18}\text{F}$ -DFA PET. Immunohistochemical staining for the FAH enzyme, which is only present in the engrafted human hepatocytes, in liver sections from these mice suggests that  $71\% \pm 3.6\%$  of the liver hepatocytes are of human origin (**Fig. 5B**). Hepatic  $^{18}\text{F}$ -DFA accumulation in these mice was indistinguishable from hepatic  $^{18}\text{F}$ -DFA accumulation in non-engrafted control FRG mice maintained on NTBC (e.g. mice whose livers only contain mouse hepatocytes) ( $p=0.06$ ; **Fig. 5C**). The behavior of  $^{18}\text{F}$ -DFA in humans will depend both on hepatic ribose salvage activity and the metabolism of  $^{18}\text{F}$ -DFA by other organs and tissues in the body. Nevertheless, this data may suggest that PET imaging with a radiotracer that measures ribose salvage activity could provide information on liver function in humans.

## **Discussion**

Various approaches have been used to monitor the liver during drug-induced acute liver injury, including liver biopsies and biochemical tests of liver function (1,6–9,13,14). There are a number of reasons why PET imaging may complement and provide additional information to these assays. Liver biopsies sample 1/50,000 to 1/100,000 of the liver, leading to significant sampling error (37–40). This may be especially true when the hepatic disease manifests heterogeneously, such as during acute liver injury (7,9). PET imaging provides a view of the entire liver and eliminates sampling error. Biochemical assessments of liver function from plasma are indirect, diluted across the entire blood volume, and confounded during acute liver failure when various processes are occurring simultaneously (41). PET imaging with  $^{18}\text{F}$ -DFA allows for the direct visualization and quantification of a critical parameter: functional hepatocytes.  $^{18}\text{F}$ -DFA is not the only radiotracer that accumulates in the liver through specific biochemical processes, and other

tracers include  $^{99m}\text{Tc}$ -labelled galactosyl human serum albumin and 2- $^{18}\text{F}$ -fluoro-2-deoxygalactose (42,43). Future studies will be required to compare  $^{18}\text{F}$ -DFA to these and other tracers in this same model.

Many treatments for acetaminophen-induced hepatotoxicity work by preventing liver damage (35,44). These treatments, exemplified by NAC, can have a profound impact on patient health but their efficacy is limited to very early after acetaminophen ingestion, before hepatocellular damage has occurred (6). Our data suggests that a threshold level of functional hepatocytes are required for survival following high dose acetaminophen. We identify that hepatic  $^{18}\text{F}$ -DFA accumulation increases specifically in the surviving mice between 7 and 21 hours post-acetaminophen treatment, suggesting a potentially important role for liver regeneration in reaching that threshold. This suggestion is consistent with preclinical studies indicating that stimulating liver regeneration can improve the survival of mice treated with high dose acetaminophen and limited clinical data suggesting that biomarkers of liver regeneration may be useful for identifying patients who will survive acetaminophen overdose without a liver transplant (11,45–48).

#### *Implications for human studies*

We demonstrate that PET imaging with  $^{18}\text{F}$ -DFA can be used to distinguish mice that will survive acetaminophen overdose from those that will not and, while appreciating important differences between mice and humans, postulate that this approach may have similar utility in people.  $^{18}\text{F}$ -DFA measures ribose salvage activity (15), and we demonstrate that in culture and engrafted into the livers of mice, human hepatocytes have similar levels of ribose salvage activity as mouse hepatocytes. However, whether the approach here works in people will depend on a number of additional factors. One factor is whether a PET scan can be performed in sufficient

time to affect clinical decision making. The mouse model we use shares many features of the clinical human disease but differs in the speed at which liver failure occurs (6,49–51). Mice can succumb to high dose acetaminophen treatment within 24 hours while humans often do not present with clear symptoms of acetaminophen overdose for at least 72 hours. Symptoms can last for months, although action is often taken within 3 – 5 days of presentation (1,6,49–52). 3 – 5 days is a short but not inconceivable time period in which to perform and analyze a PET scan. Clinical PET protocols have been developed for imaging patients within 24 hours of presentation (53–57). The majority of liver transplants in America are performed at less than 100 sites (58), suggesting that if a rapid protocol were developed, it would only need to be instituted at a limited number of specialized centers.

Another important factor to consider when translating this approach to humans is the patient-to-patient variability in hepatic  $^{18}\text{F}$ -DFA accumulation. A patient suffering from acetaminophen overdose would likely only be imaged once. High patient-to-patient variability in hepatic  $^{18}\text{F}$ -DFA accumulation would make it challenging to differentiate between, for example, an individual with naturally low hepatic  $^{18}\text{F}$ -DFA accumulation from an individual with low hepatic  $^{18}\text{F}$ -DFA accumulation due to a dramatic loss of hepatocytes.  $^{18}\text{F}$ -DFA has not been tested yet in humans so we cannot report on patient-to-patient variability. However we show that the entropy present in the PET images has the lowest coefficient of variation among the variables analyzed within the cohort of treated mice and may represent an important quantity to evaluate if this approach is tested in humans.

We demonstrate that  $^{18}\text{F}$ -DFA PET imaging provides a quantitative, whole organ measure of the functional hepatocyte density following acetaminophen induced acute liver injury. As with any liver test, we do not expect that these results by themselves will be absolutely predictive of acute liver failure in humans. We do anticipate that in combination with other measures, including those related to non-hepatic organ failure, the information gained through this PET assay may

improve the allocation of livers for transplant. Acetaminophen overdose is the most prevalent, though not the only, cause of acute liver failure (2,6,50,59). Other causes of acute liver injury include Hepatitis B, Wilson Disease, and idiosyncratic drug-induced liver injury caused by such drugs as the EGFR inhibitor gefitinib, the anti-retroviral maraviroc, and the epilepsy medication levetiracetam (2,3). Nothing about the biochemistry of hepatic  $^{18}\text{F}$ -DFA accumulation suggests that the results demonstrated here would be specific for acetaminophen induced acute liver injury. Thus it will be interesting to test this PET imaging approach in other models of acute and chronic liver injury.

## **Disclosures**

PMC and ONW are inventors on a patent, held by the Regents of the University of California, that describes the  $^{18}\text{F}$ -DFA radiotracer.

## **Acknowledgements**

We thank members of the Crump Preclinical Imaging Technology Center, the Crump Cyclotron and Radiochemistry Technology Center, and the UCLA Translational Pathology Core Laboratory for their assistance. We thank Ralph and Marjorie Crump for their donation to the UCLA Crump Institute for Molecular Imaging. We thank Dr. Ali Zarrinpar for helpful discussions on acute liver injury in humans. We thank Drs. Claire Faltermeier and John Van Arnam for helpful suggestions on the manuscript. This work was supported by NIH/NCATS Grant #UL1TR000124 (to P.M.C.), CIRM Grant #TR4-06831 (to G.S.L.), NIH/NINDS Grant #1R01NS100979-01 (to G.S.L.), the Parker Institute for Cancer Immunotherapy (PICI) Grant #20163828 (to O.N.W.), and the Broad Stem Cell Research Center at UCLA.

## References

1. Larson AM, Polson J, Fontana RJ, et al. Acetaminophen-induced acute liver failure: results of a United States multicenter, prospective study. *Hepatology*. 2005;42:1364-1372.
2. Reuben A, Koch DG, Lee WM, Acute Liver Failure Study Group. Drug-induced acute liver failure: results of a U.S. multicenter, prospective study. *Hepatology*. 2010;52:2065-2076.
3. Bunchorntavakul C, Reddy KR. Drug Hepatotoxicity: Newer Agents. *Clin Liver Dis*. 2017;21:115-134.
4. Robles-Diaz M, Lucena MI, Kaplowitz N, et al. Use of Hy's law and a new composite algorithm to predict acute liver failure in patients with drug-induced liver injury. *Gastroenterology*. 2014;147:109-118.e5.
5. Björnsson E, Olsson R. Outcome and prognostic markers in severe drug-induced liver disease. *Hepatology*. 2005;42:481-489.
6. Lancaster EM, Hiatt JR, Zarrinpar A. Acetaminophen hepatotoxicity: an updated review. *Arch Toxicol*. 2015;89:193-199.
7. Singhal A, Vadlamudi S, Stokes K, et al. Liver histology as predictor of outcome in patients with acute liver failure. *Transpl Int*. 2012;25:658-662.
8. Scotto J, Opolon P, Etévé J, Vergoz D, Thomas M, Caroli J. Liver biopsy and prognosis in acute liver failure. *Gut*. 1973;14:927-933.
9. Hanau C, Munoz SJ, Rubin R. Histopathological heterogeneity in fulminant hepatic failure. *Hepatology*. 1995;21:345-351.
10. Brown AT, Ou X, James LP, et al. Correlation of MRI findings to histology of acetaminophen toxicity in the mouse. *Magn Reson Imaging*. 2012;30:283-289.
11. Shakil AO, Jones BC, Lee RG, Federle MP, Fung JJ, Rakela J. Prognostic value of abdominal CT scanning and hepatic histopathology in patients with acute liver failure. *Dig Dis Sci*. 2000;45:334-339.
12. Romero M, Palmer SL, Kahn JA, et al. Imaging appearance in acute liver failure: correlation with clinical and pathology findings. *Dig Dis Sci*. 2014;59:1987-1995.
13. McPhail MJW, Farne H, Senvar N, Wendon JA, Bernal W. Ability of King's College Criteria and Model for End-Stage Liver Disease Scores to Predict Mortality of Patients With Acute Liver Failure: A Meta-analysis. *Clin Gastroenterol Hepatol*. 2016;14:516-525.e5; quiz e43-e45.
14. Bailey B, Amre DK, Gaudreault P. Fulminant hepatic failure secondary to acetaminophen poisoning: a systematic review and meta-analysis of prognostic criteria determining the need for liver transplantation. *Crit Care Med*. 2003;31:299-305.

15. Clark PM, Flores G, Evdokimov NM, et al. Positron emission tomography probe demonstrates a striking concentration of ribose salvage in the liver. *Proc Natl Acad Sci U S A*. 2014;111:E2866-2874.
16. Evdokimov NM, Clark PM, Flores G, et al. Development of 2-Deoxy-2-[<sup>18</sup>F]fluororibose for Positron Emission Tomography Imaging Liver Function in Vivo. *J Med Chem*. 2015;58:5538-5547.
17. Collins J, Waldmann CM, Drake C, et al. Production of diverse PET probes with limited resources: 24 <sup>18</sup>F-labeled compounds prepared with a single radiosynthesizer. *Proc Natl Acad Sci U S A*. 2017;114:11309-11314.
18. Sommer C, Straehle C, Köthe U, Hamprecht FA. Ilastik: Interactive learning and segmentation toolkit. In: 2011 IEEE International Symposium on Biomedical Imaging: From Nano to Macro. ; 2011:230-233.
19. Schneider CA, Rasband WS, Eliceiri KW. NIH Image to ImageJ: 25 years of image analysis. *Nat Methods*. 2012;9:671-675.
20. Shu CJ, Radu CG, Shelly SM, et al. Quantitative PET reporter gene imaging of CD8+ T cells specific for a melanoma-expressed self-antigen. *Int Immunol*. 2009;21:155-165.
21. Hur KY, So J-S, Ruda V, et al. IRE1 $\alpha$  activation protects mice against acetaminophen-induced hepatotoxicity. *J Exp Med*. 2012;209:307-318.
22. McGill MR, Sharpe MR, Williams CD, Taha M, Curry SC, Jaeschke H. The mechanism underlying acetaminophen-induced hepatotoxicity in humans and mice involves mitochondrial damage and nuclear DNA fragmentation. *J Clin Invest*. 2012;122:1574-1583.
23. Kheradpezhohu E, Ma L, Morphett A, Barritt GJ, Rychkov GY. TRPM2 channels mediate acetaminophen-induced liver damage. *Proc Natl Acad Sci U S A*. 2014;111:3176-3181.
24. Agarwal S, Holton KL, Lanza R. Efficient differentiation of functional hepatocytes from human embryonic stem cells. *Stem Cells*. 2008;26:1117-1127.
25. Zhang J, Song S, Pang Q, et al. Serotonin deficiency exacerbates acetaminophen-induced liver toxicity in mice. *Sci Rep*. 2015;5:8098.
26. Phelps ME. Positron emission tomography provides molecular imaging of biological processes. *Proc Natl Acad Sci U S A*. 2000;97:9226-9233.
27. Gambhir SS. Molecular imaging of cancer with positron emission tomography. *Nat Rev Cancer*. 2002;2:683-693.
28. Iozzo P, Geisler F, Oikonen V, et al. Insulin stimulates liver glucose uptake in humans: an <sup>18</sup>F-FDG PET Study. *J Nucl Med*. 2003;44:682-689.
29. Azuma H, Paulk N, Ranade A, et al. Robust expansion of human hepatocytes in Fah<sup>-/-</sup>/Rag2<sup>-/-</sup>/Il2rg<sup>-/-</sup> mice. *Nat Biotechnol*. 2007;25:903-910.

30. Tixier F, Le Rest CC, Hatt M, et al. Intratumor heterogeneity characterized by textural features on baseline <sup>18</sup>F-FDG PET images predicts response to concomitant radiochemotherapy in esophageal cancer. *J Nucl Med*. 2011;52:369-378.
31. Cook GJR, Yip C, Siddique M, et al. Are pretreatment <sup>18</sup>F-FDG PET tumor textural features in non-small cell lung cancer associated with response and survival after chemoradiotherapy? *J Nucl Med*. 2013;54:19-26.
32. Cook GJR, Siddique M, Taylor BP, Yip C, Chicklore S, Goh V. Radiomics in PET: principles and applications. *Clin Transl Imaging*. 2014;2:269-276.
33. Clark PM, Ebiana VA, Gosa L, Cloughesy TF, Nathanson DA. Harnessing Preclinical Molecular Imaging to Inform Advances in Personalized Cancer Medicine. *J Nucl Med*. 2017;58:689-696.
34. Soeda J, Mouralidarane A, Ray S, et al. The  $\beta$ -adrenoceptor agonist isoproterenol rescues acetaminophen-injured livers through increasing progenitor numbers by Wnt in mice. *Hepatology*. 2014;60:1023-1034.
35. Ni H-M, Bockus A, Boggess N, Jaeschke H, Ding W-X. Activation of autophagy protects against acetaminophen-induced hepatotoxicity. *Hepatology*. 2012;55:222-232.
36. James LP, McCullough SS, Lamps LW, Hinson JA. Effect of N-acetylcysteine on acetaminophen toxicity in mice: relationship to reactive nitrogen and cytokine formation. *Toxicol Sci*. 2003;75:458-467.
37. Nord HJ. Biopsy diagnosis of cirrhosis: blind percutaneous versus guided direct vision techniques--a review. *Gastrointest Endosc*. 1982;28:102-104.
38. Jeffers LJ, Cortes RA, Bejarano PA, et al. Prospective Evaluation of FIBROSpect II for Fibrosis Detection in Hepatitis C and B Patients Undergoing Laparoscopic Biopsy. *Gastroenterol Hepatol*. 2007;3:367-376.
39. Soloway RD, Baggenstoss AH, Schoenfield LJ, Summerskill WH. Observer error and sampling variability tested in evaluation of hepatitis and cirrhosis by liver biopsy. *Am J Dig Dis*. 1971;16:1082-1086.
40. Abdi W, Millan JC, Mezey E. Sampling variability on percutaneous liver biopsy. *Arch Intern Med*. 1979;139:667-669.
41. John Dubray B, Zarrinpar A. Quantification of hepatic functional capacity: a call for standardization. *Expert Rev Gastroenterol Hepatol*. 2016;10:9-11.
42. Vera DR, Krohn KA, Stadalnik RC, Scheibe PO. Tc-<sup>99m</sup>-galactosyl-neoglycoalbumin: in vivo characterization of receptor-mediated binding to hepatocytes. *Radiology*. 1984;151:191-196.
43. Sørensen M, Frisch K, Bender D, Keiding S. The potential use of 2-[<sup>18</sup>F]fluoro-2-deoxy-D-galactose as a PET/CT tracer for detection of hepatocellular carcinoma. *Eur J Nucl Med Mol Imaging*. 2011;38:1723-1731.

44. Lauterburg BH, Corcoran GB, Mitchell JR. Mechanism of action of *N*-acetylcysteine in the protection against the hepatotoxicity of acetaminophen in rats in vivo. *J Clin Invest*. 1983;71:980-991.
45. Schmidt LE, Dalhoff K. Alpha-fetoprotein is a predictor of outcome in acetaminophen-induced liver injury. *Hepatology*. 2005;41:26-31.
46. Horn KD, Wax P, Schneider SM, et al. Biomarkers of liver regeneration allow early prediction of hepatic recovery after acute necrosis. *Am J Clin Pathol*. 1999;112:351-357.
47. Hu B, Colletti LM. Stem cell factor and c-kit are involved in hepatic recovery after acetaminophen-induced liver injury in mice. *Am J Physiol Gastrointest Liver Physiol*. 2008;295:G45-G53.
48. Donahower BC, McCullough SS, Hennings L, et al. Human recombinant vascular endothelial growth factor reduces necrosis and enhances hepatocyte regeneration in a mouse model of acetaminophen toxicity. *J Pharmacol Exp Ther*. 2010;334:33-43.
49. Clark R, Borirakchanyavat V, Davidson AR, et al. Hepatic damage and death from overdose of paracetamol. *Lancet*. 1973;1:66-70.
50. Yoon E, Babar A, Choudhary M, Kutner M, Pysopoulos N. Acetaminophen-Induced Hepatotoxicity: a Comprehensive Update. *J Clin Transl Hepatol*. 2016;4:131-142.
51. Ostapowicz G, Fontana RJ, Schiødt FV, et al. Results of a prospective study of acute liver failure at 17 tertiary care centers in the United States. *Ann Intern Med*. 2002;137:947-954.
52. O'Grady JG, Wendon J, Tan KC, et al. Liver transplantation after paracetamol overdose. *BMJ*. 1991;303:221-223.
53. Markus R, Reutens DC, Kazui S, et al. Topography and temporal evolution of hypoxic viable tissue identified by <sup>18</sup>F-fluoromisonidazole positron emission tomography in humans after ischemic stroke. *Stroke J Cereb Circ*. 2003;34:2646-2652.
54. Read SJ, Hirano T, Abbott DF, et al. Identifying hypoxic tissue after acute ischemic stroke using PET and <sup>18</sup>F-fluoromisonidazole. *Neurology*. 1998;51:1617-1621.
55. Markus R, Reutens DC, Kazui S, et al. Hypoxic tissue in ischaemic stroke: persistence and clinical consequences of spontaneous survival. *Brain J Neurol*. 2004;127:1427-1436.
56. Lee G-H, Kim JS, Oh SJ, Kang D-W, Kim JS, Kwon SU. <sup>18</sup>F-fluoromisonidazole (FMISO) Positron Emission Tomography (PET) Predicts Early Infarct Growth in Patients with Acute Ischemic Stroke. *J Neuroimaging*. 2015;25:652-655.
57. Heiss WD, Kracht L, Grond M, et al. Early [<sup>11</sup>C]Flumazenil/H<sub>2</sub>O positron emission tomography predicts irreversible ischemic cortical damage in stroke patients receiving acute thrombolytic therapy. *Stroke J Cereb Circ*. 2000;31:366-369.
58. Brown RS, Russo MW, Lai M, et al. A survey of liver transplantation from living adult donors in the United States. *N Engl J Med*. 2003;348:818-825.

59. Nourjah P, Ahmad SR, Karwoski C, Willy M. Estimates of acetaminophen (Paracetamol)-associated overdoses in the United States. *Pharmacoepidemiol Drug Saf.* 2006;15:398-405.

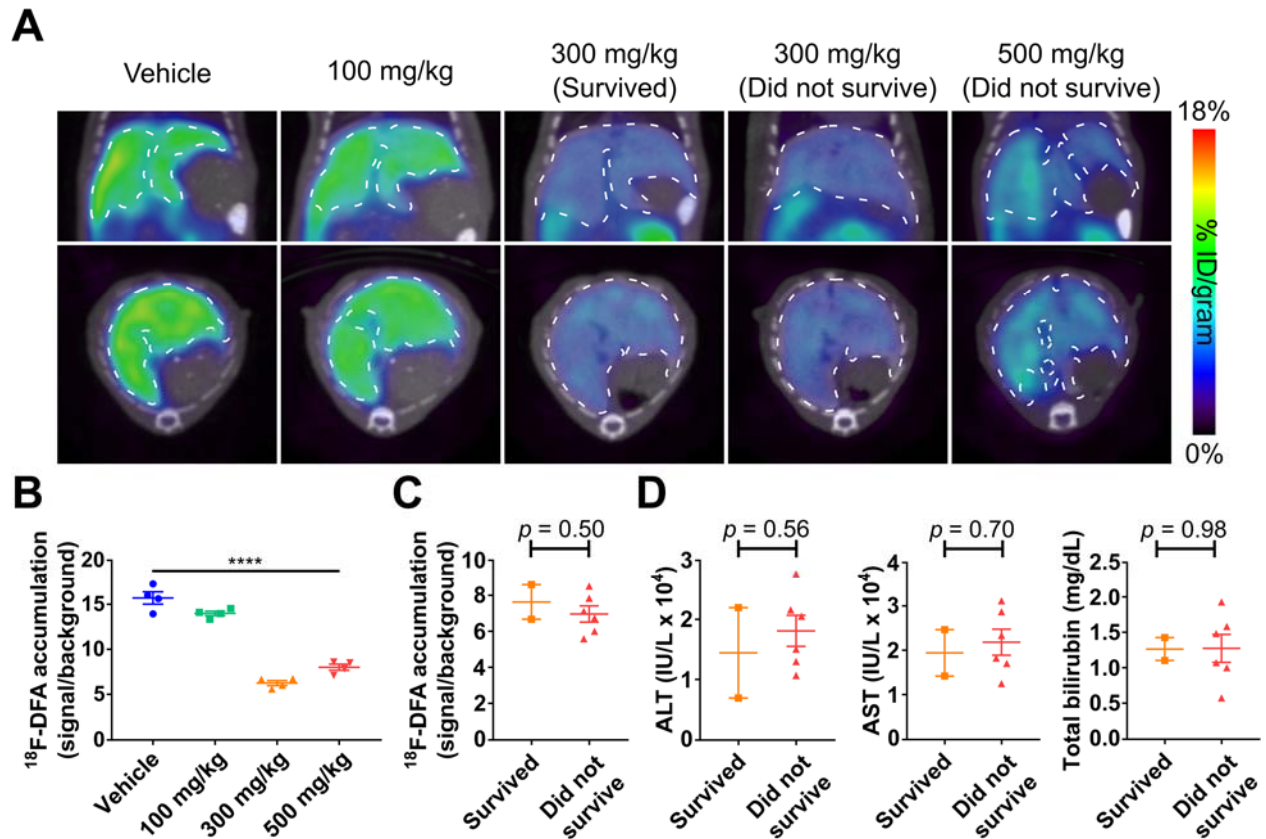


**Figure 1:** PET imaging with  $^{18}\text{F}$ -DFA 7 hours after acetaminophen treatment can distinguish low and high dose acetaminophen-treated mice but cannot distinguish mice that will survive high dose acetaminophen from those that will not. (A) Representative transverse and coronal  $^{18}\text{F}$ -DFA PET/CT images of mice, 7 hours after treatment with saline vehicle or acetaminophen. Dotted white lines encircle the livers. Quantification of hepatic  $^{18}\text{F}$ -DFA accumulation in mice, 7 hours after treatment with saline vehicle or acetaminophen, plotted by (B) acetaminophen dose or (C) survival status. (D) ALT, AST, and total bilirubin levels from the serum of mice treated for 7 hours with high dose acetaminophen, plotted by survival status. All doses:  $n=4$ ; survived:  $n=2$ ; did not survive:  $n=6$ . One-way ANOVA for (B); unpaired t tests for (C) and (D). \*\*\*\*:  $p<0.0001$ .

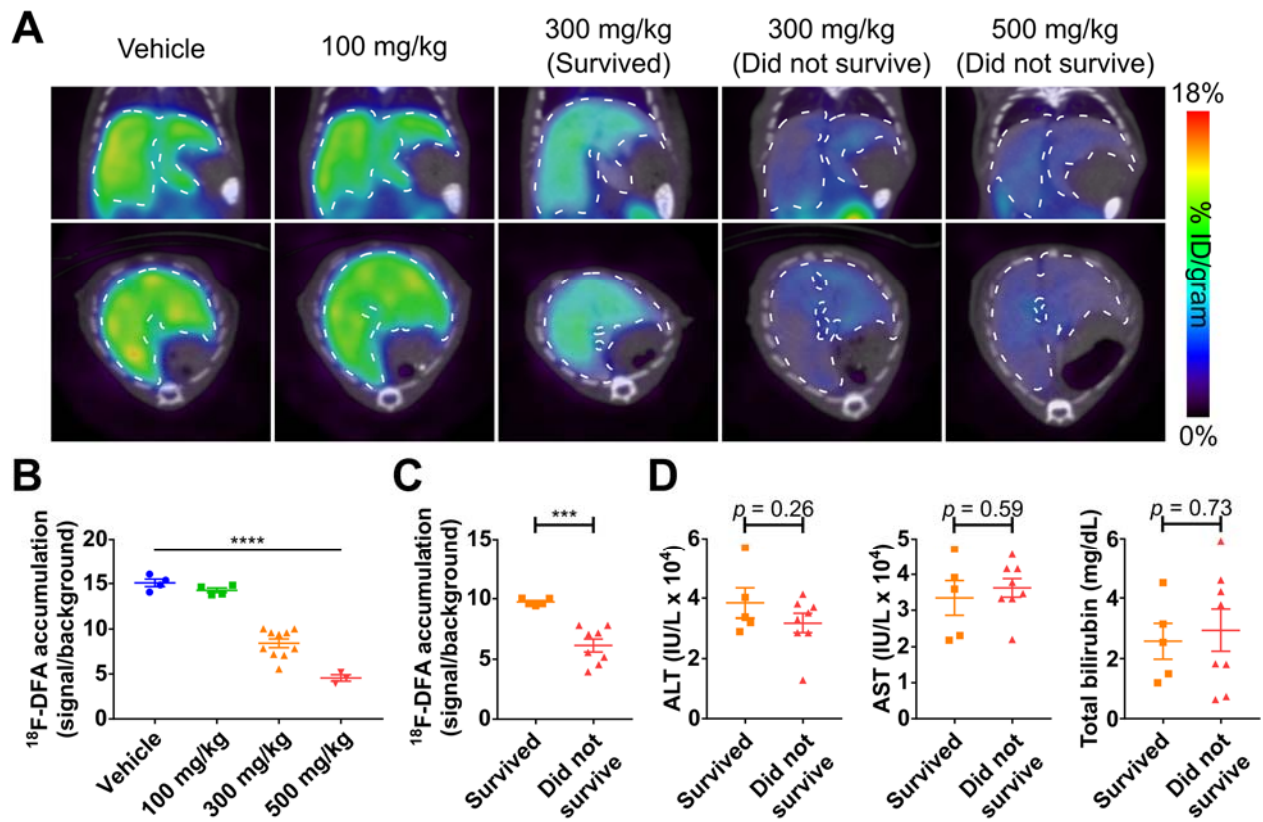


**Figure 2:** PET imaging with  $^{18}\text{F}$ -DFA 21 hours after acetaminophen treatment can distinguish mice that will survive high dose acetaminophen from mice that will not. (A) Representative transverse and coronal  $^{18}\text{F}$ -DFA PET/CT images of mice, 21 hours after treatment with saline vehicle or acetaminophen. Quantification of hepatic  $^{18}\text{F}$ -DFA accumulation in mice, 21 hours after treatment with saline vehicle or acetaminophen, plotted by (B) acetaminophen dose or (C) survival status. (D) ALT, AST, and total bilirubin levels from the serum of mice treated with high dose acetaminophen for 21 hours, plotted by survival status. Vehicle and 100 mg/kg:  $n=4$ ; 300 mg/kg:  $n=10$ ; 500 mg/kg:  $n=3$ ; survived:  $n=5$ ; did not survive:  $n=8$ . One-way ANOVA for (B); unpaired t tests for (C) and (D). \*\*\*:  $p < 0.001$ ; \*\*\*\*:  $p < 0.0001$ .

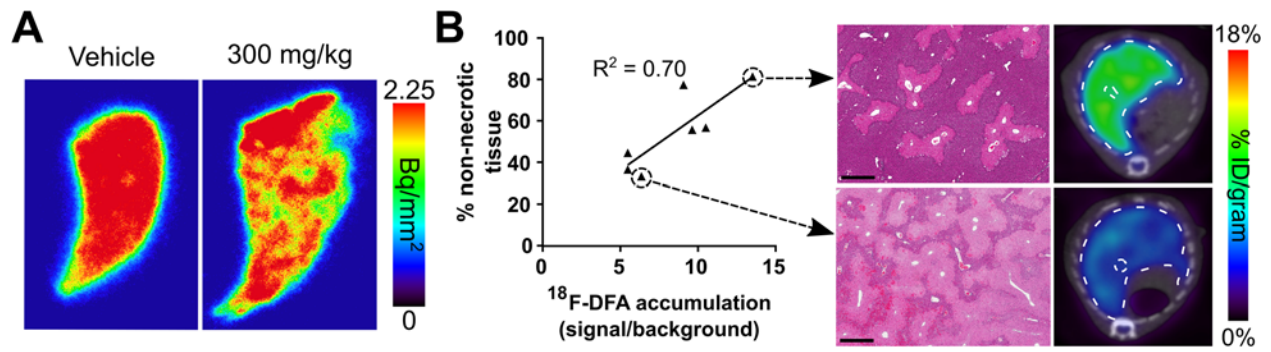


**Figure 3:**  $^{18}\text{F}$ -DFA accumulation measures functional liver tissue following acetaminophen-induced liver injury. (A) Digital autoradiography of liver sections from mice treated with saline vehicle or 300 mg/kg acetaminophen for 7 hours and injected with  $^{18}\text{F}$ -DFA.  $n=2$ . (B) A correlation between percent non-necrotic tissue and hepatic  $^{18}\text{F}$ -DFA accumulation in mice treated with 300 mg/kg acetaminophen for 21 hours (left). Representative H&E stained liver sections and transverse  $^{18}\text{F}$ -DFA PET/CT images (right). Scale bars represent 500 microns.  $n=7$ .

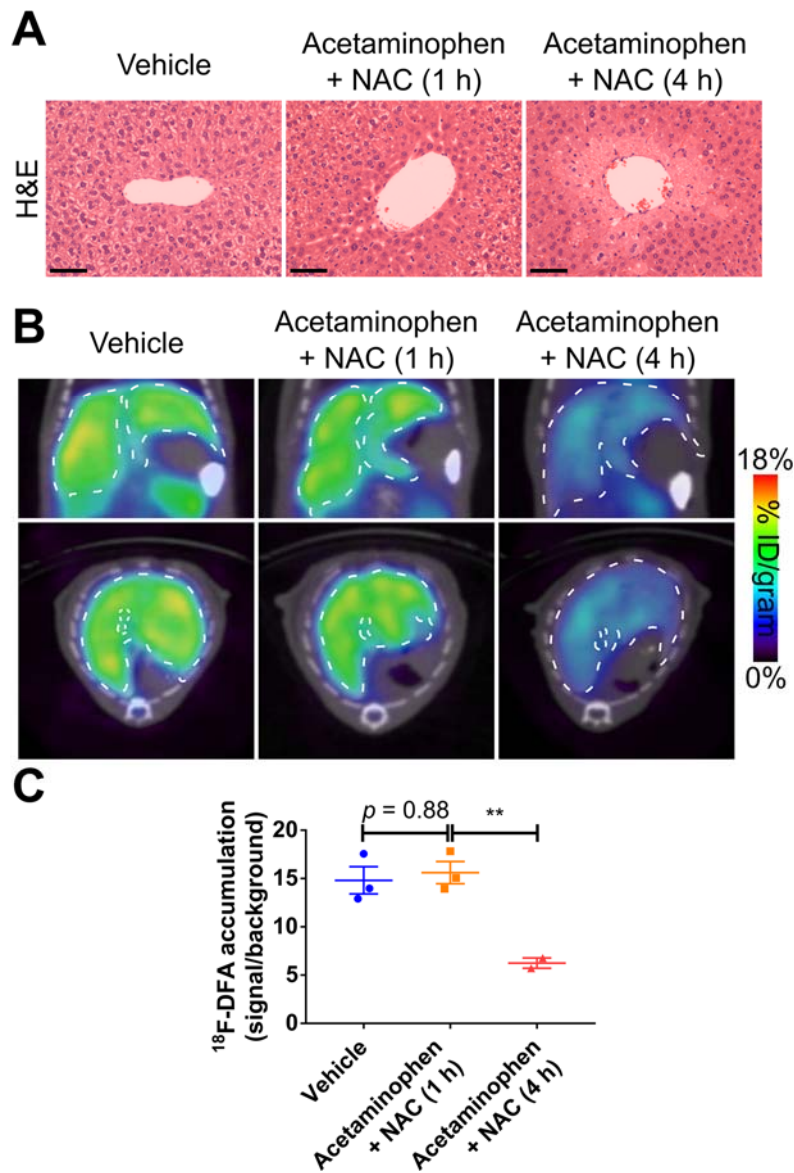


**Figure 4:** PET imaging with  $^{18}\text{F}$ -DFA can monitor the efficacy of treatments for acetaminophen overdose. (A) Representative H&E-stained liver sections, (B) representative transverse and coronal  $^{18}\text{F}$ -DFA PET/CT images, and (C) quantification of hepatic  $^{18}\text{F}$ -DFA accumulation of mice treated for 21 h with saline vehicle, with *N*-acetylcysteine (NAC) 1 h after 300 mg/kg acetaminophen, or with NAC 4 h after 300 mg/kg acetaminophen. Scale bars represent 100 microns. Vehicle:  $n=3$ ; Acetaminophen + NAC (1 h):  $n=3$ ; Acetaminophen + NAC (4 h):  $n=2$ . One-way ANOVA with Tukey correction. \*\*:  $p<0.01$ .

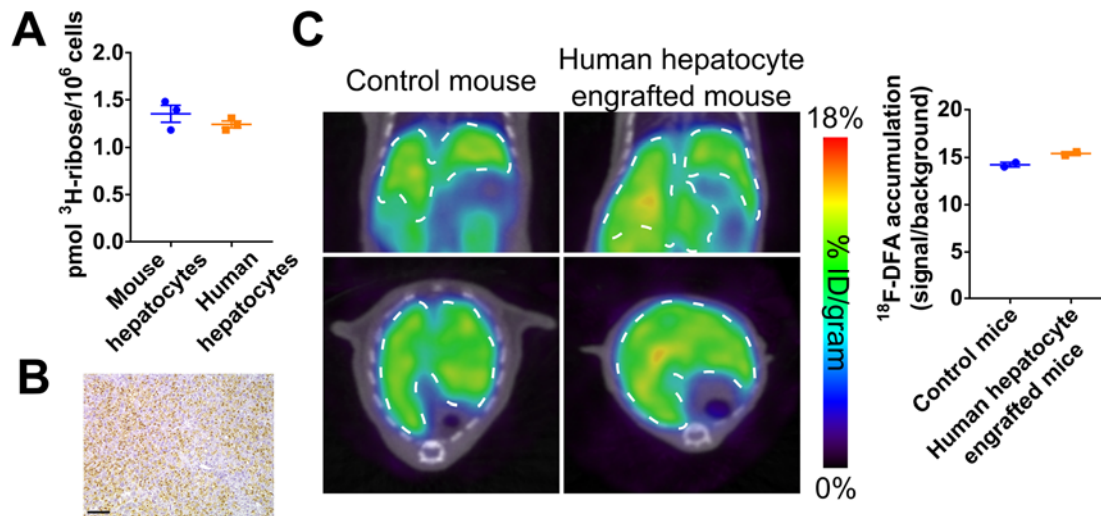


**Figure 5:** Ribose salvage activity is similar between mouse and human hepatocytes. (A) <sup>3</sup>H-ribose consumption in mouse and human hepatocytes in cell culture. *n*=3. (B) Representative mouse liver tissue section from a mouse treated with human hepatocytes, immunostained for FAH. Scale bar represents 100 microns. (C) Representative coronal and transverse <sup>18</sup>F-DFA PET/CT images of control mice and mice whose livers are engrafted with human hepatocytes (left). Quantification of hepatic <sup>18</sup>F-DFA accumulation in these mice (right). *n*=2.

# Supplemental information

## Non-invasive imaging of drug-induced liver injury with $^{18}\text{F}$ -DFA PET

Jessica R. Salas<sup>1,2</sup>, Bao Ying Chen<sup>1,2</sup>, Alicia Wong<sup>1,2</sup>, Sergio Duarte<sup>3</sup>, Stephanie A. K. Angarita<sup>3</sup>,  
Gerald S. Lipshutz<sup>1,4,5</sup>, Owen N. Witte<sup>1,4,6</sup>, Peter M. Clark<sup>1,2,4,†</sup>

*<sup>1</sup> Department of Molecular and Medical Pharmacology, <sup>2</sup> Crump Institute for Molecular Imaging, <sup>3</sup> Department of Surgery, <sup>4</sup> Eli and Edythe Broad Center of Regenerative Medicine and Stem Cell Research, <sup>5</sup> Intellectual and Developmental Disabilities Research Center, <sup>6</sup> Department of Microbiology, Immunology and Molecular Genetics, University of California, Los Angeles CA 90095*

## Supplemental Methods

*FRG mouse model of acute liver failure:* FRG male mice (12 weeks old) were maintained on drinking water supplemented with 16 mg/L NTBC (Yecuris) and Bactrim from birth and then switched to drinking water supplemented only with Bactrim.

*Human hepatocyte engraftment into FRG mice:*

Human hepatocytes: Fresh human hepatocytes (Yecuris) were prepared according to the distributor's protocol. Hepatocytes were washed by centrifugation (140xg, 5 min, 4 °C) and resuspended in HCM medium (Lonza). Cells were counted and viability determined by an automated cell counter (Nexcelom Bioscience), and the hepatocytes were resuspended in HCM medium at a concentration of  $1 \times 10^6$  cells/300  $\mu$ L. Hepatocytes were kept on ice until transplanted into mice.

Hepatocyte transplantation into FRG mice: FRG mice (Yecuris) were purchased and bred at UCLA. Prior to transplantation, FRG mice were provided drinking water supplemented with 16 mg/L NTBC (Yecuris) and Bactrim. 24 h before the hepatocyte transplantation, mice were anesthetized with isoflurane and inoculated with  $1.25 \times 10^9$  pfu / 25g body weight of CuRx uPA Liver Tx Enhancer (Yecuris) via retro-orbital injection. The day of the transplantation, the mice were anesthetized with isoflurane, and the area of incision in the left subcostal region was clipped of hair and washed with 70% EtOH and povidone-iodine solution. A 0.5 cm transverse left subcostal incision was made through the skin, muscle, and peritoneum. The spleen was identified and gently retracted out of the incision onto sterile gauze. A small part of the spleen was tied gently using a 4-0 silk taking care not to avulse the nub of spleen.  $1 \times 10^6$  hepatocytes were slowly injected into the spleen using a 28.5 G needle syringe through the tied off splenic nub and loop of suture so as to minimize bleeding from the puncture site. The suture was cut and the spleen was returned to the abdomen. The peritoneum and muscle layers and subsequently, the skin,

were closed separately using a 4-0 Vicryl suture. The mouse was recovered on a heated mat in a clean recovery cage.

NTBC cycling: 24 hours prior to the hepatocyte transplantation, the drinking water was switched to water without NTBC and was maintained that way for 7 days, after which mice were provided with drinking water supplemented with 8 mg/L NTBC for 3 days. This cycle was repeated for a total of 60 days. Next, mice were provided with drinking water without NTBC for 3 weeks followed by drinking water supplemented with 8 mg/L NTBC for 3 days. From 4 – 6 months, mice were only provided with drinking water without NTBC unless the mice lost >20% of their body weight, in which case the mice were provided with drinking water supplemented with 8 mg/L NTBC for 1 – 3 days. Supplemental nutritional support was provided by placing STAT liquid (PRN Pharmacal) in the mouse cages.

*Mouse numbers:* 7 hours post acetaminophen-treatment, imaged with  $^{18}\text{F}$ -DFA and analyzed for blood chemistries – All doses:  $n = 4$ ; survived:  $n = 2$ ; did not survive:  $n = 6$ . 21 hours post acetaminophen-treatment, imaged with  $^{18}\text{F}$ -DFA and analyzed for blood chemistries – Vehicle and 100 mg/kg:  $n = 4$ ; 300 mg/kg:  $n = 10$ ; 500 mg/kg:  $n = 3$ ; survived:  $n = 5$ ; did not survive:  $n = 8$ . Autoradiography experiments:  $n = 2$ . Hepatic  $^{18}\text{F}$ -DFA accumulation and non-necrotic tissue correlation study:  $n = 7$ . Vehicle or acetaminophen-treated mice treated with NAC – Vehicle:  $n = 3$ ; Acetaminophen + NAC (1 h):  $n = 3$ ; Acetaminophen + NAC (4 h):  $n = 2$ . Human hepatocyte experiments – Control FRG mice:  $n = 2$ ; human hepatocyte-engrafted FRG mice:  $n = 2$ . Kaplan Meier curve – Vehicle:  $n = 8$ ; 100 mg/kg:  $n = 8$ ; 300 mg/kg:  $n = 14$ ; 500 mg/kg:  $n = 10$ . Serum AST and ALT values – 7 hours, all doses:  $n = 6$ ; 21 hours, vehicle:  $n = 4$ ; 100 and 300 mg/kg:  $n = 6$ ; 500 mg/kg:  $n = 5$ . Histology:  $n = 2$ . Acetaminophen-treated mice imaged with  $^{18}\text{F}$ -FDG and analyzed for blood chemistries – Vehicle and 7 hours:  $n = 3$ ; 21 hours:  $n = 4$ . FRG mouse liver injury experiments –  $n = 6$ , imaged before and after withdrawal of NTBC.

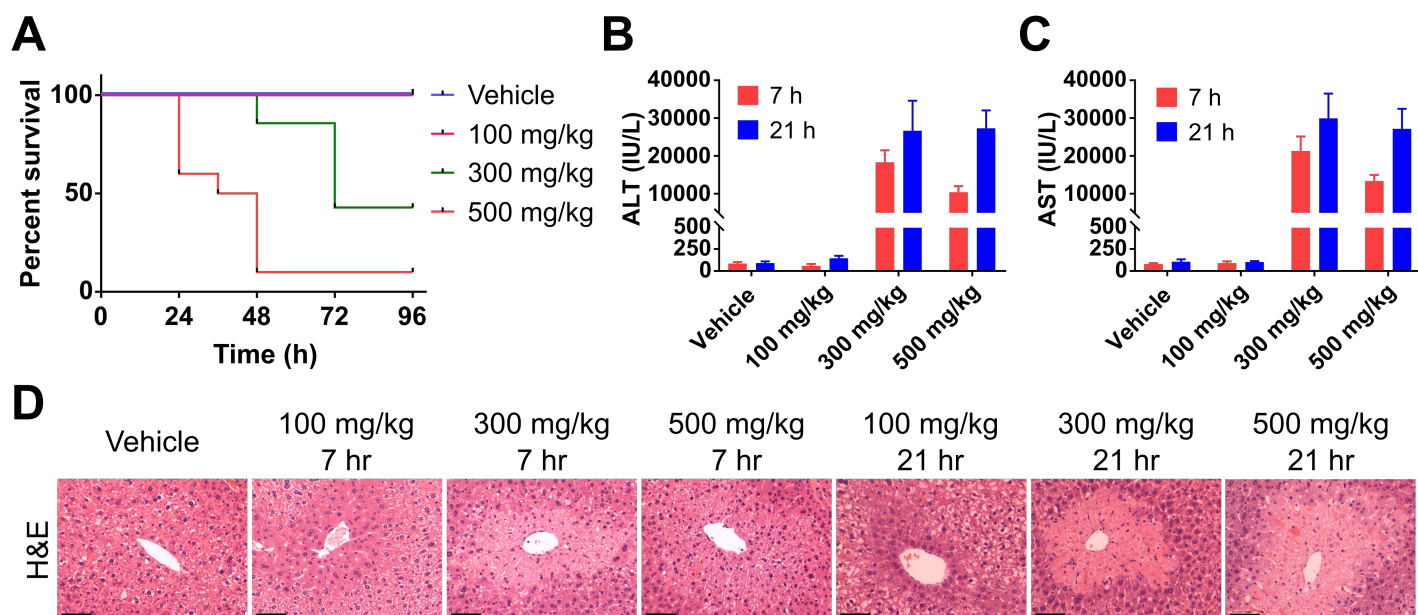


**Figure S1:** A mouse model of drug-induced liver injury. (A) A Kaplan Meier curve displaying percent survival after treating mice with saline vehicle or 100, 300, or 500 mg/kg acetaminophen. Vehicle:  $n=8$ ; 100 mg/kg:  $n=8$ ; 300 mg/kg:  $n=14$ ; 500 mg/kg:  $n=10$ . (B) Serum ALT and (C) AST values from mice treated with saline vehicle or 100, 300, or 500 mg/kg acetaminophen for 7 and 21 h. 7 hours, all doses:  $n=6$ ; 21 hours, vehicle:  $n=4$ ; 100 and 300 mg/kg:  $n=6$ ; 500 mg/kg:  $n=5$ . (D) H&E stained liver sections from mice treated with saline vehicle or 100, 300, or 500 mg/kg acetaminophen for 7 and 21 h. Scale bars represent 100 microns.

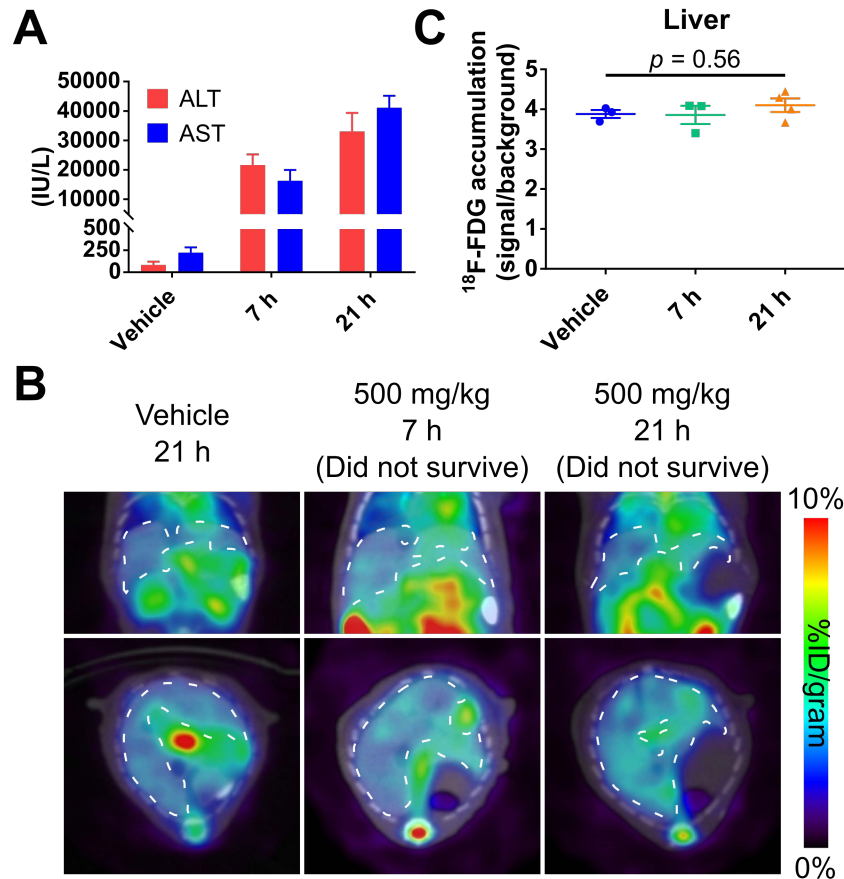


**Figure S2:** PET imaging with  $^{18}\text{F}$ -FDG cannot distinguish vehicle-treated from high dose acetaminophen-treated mice. (A) Serum ALT and AST values from mice treated with saline vehicle or 500 mg/kg acetaminophen for 7 and 21 h. Vehicle and 7 hours:  $n=3$ ; 21 hours:  $n=4$ . (B) Representative coronal and transverse  $^{18}\text{F}$ -FDG PET images of mice treated with saline vehicle or 500 mg/kg acetaminophen for 7 and 21 h. (C) Quantification of hepatic  $^{18}\text{F}$ -FDG PET accumulation in mice treated with saline vehicle or 500 mg/kg acetaminophen for 7 and 21 h. Vehicle and 7 hours:  $n=3$ ; 21 hours:  $n=4$ . One-way ANOVA.

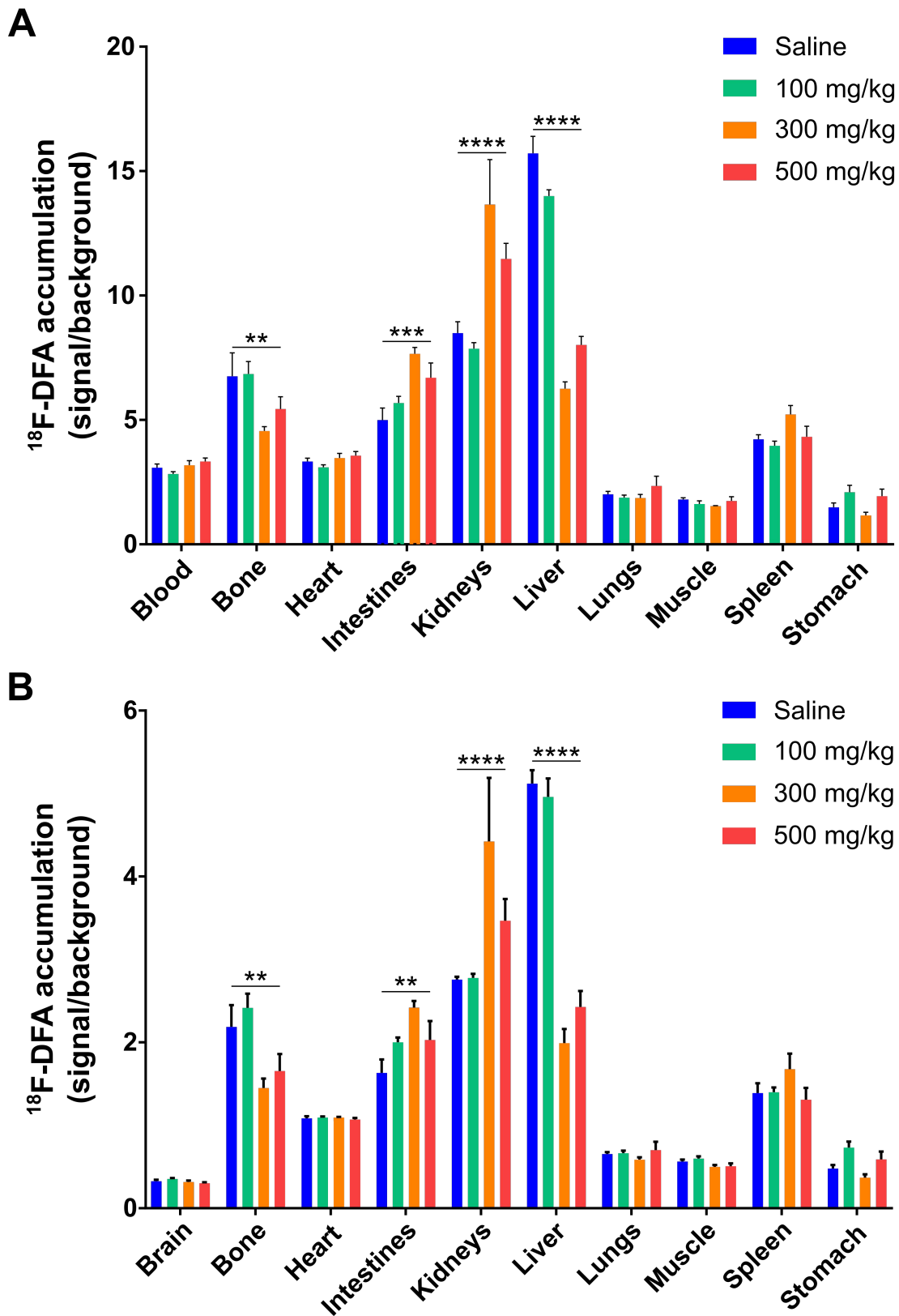


**Figure S3:** High dose (300 and 500 mg/kg) acetaminophen treatments alter the biodistribution of  $^{18}\text{F}$ -DFA accumulation. (A)  $^{18}\text{F}$ -DFA accumulation in various organs, normalized to brain  $^{18}\text{F}$ -DFA accumulation. (B)  $^{18}\text{F}$ -DFA accumulation in various organs, normalized to image-derived blood  $^{18}\text{F}$ -DFA levels. All doses:  $n=4$ . Two-way ANOVA with Dunnett correction. \*\*:  $p < 0.01$ , \*\*\*:  $p < 0.001$ , \*\*\*\*:  $p < 0.0001$ .

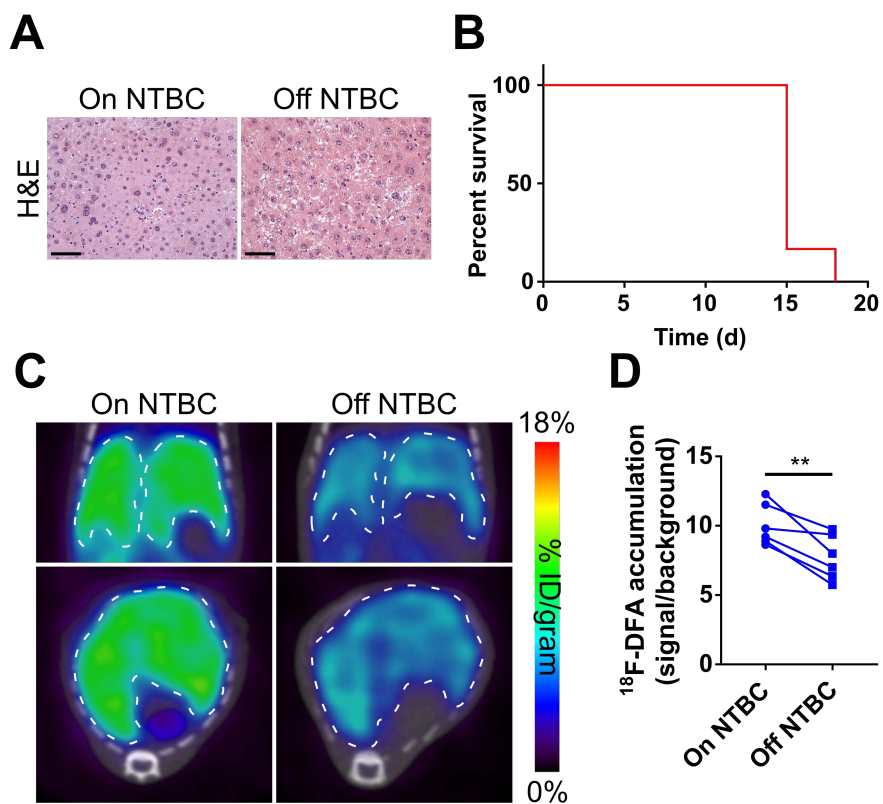


**Figure S4:** PET imaging with  $^{18}\text{F}$ -DFA can distinguish healthy mice from mice in acute liver failure induced by a toxic metabolite. (A) H&E stained liver sections from mice maintained on NTBC or withdrawn from NTBC for 2 weeks. (B) A Kaplan Meier curve displaying percent survival of FRG mice following withdrawal of NTBC. (C) Representative transverse and coronal  $^{18}\text{F}$ -DFA PET/CT images, immediately prior to and 2 weeks after withdrawal of NTBC. Dotted white lines encircle the livers. (D) Quantification of hepatic  $^{18}\text{F}$ -DFA accumulation in mice immediately prior to and 2 weeks after withdrawal of NTBC.  $n=6$ . Unpaired t test. Scale bars represent 100 microns. \*\*:  $p<0.01$ .

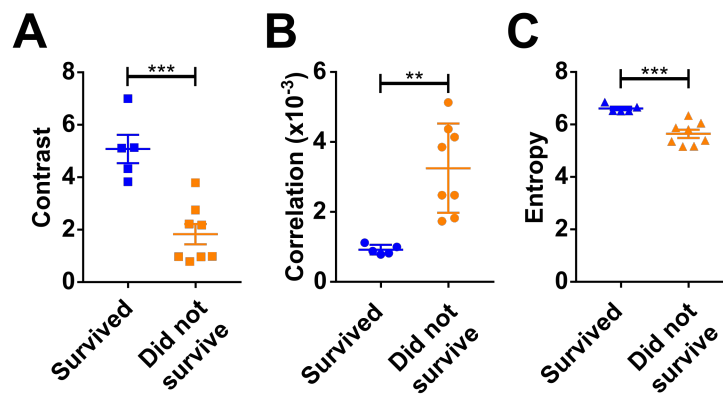


**Figure S5:** PET imaging with  $^{18}\text{F}$ -DFA 21 hours after acetaminophen treatment can distinguish mice that will survive high dose acetaminophen from mice that will not. Quantification of hepatic  $^{18}\text{F}$ -DFA (A) contrast, (B) correlation, and (C) entropy values in mice, 21 hours after treatment with high dose acetaminophen, plotted by survival status. Survived:  $n=5$ ; did not survive:  $n=8$ . Unpaired t tests. \*\*:  $p < 0.01$ ; \*\*\*:  $p < 0.001$ .

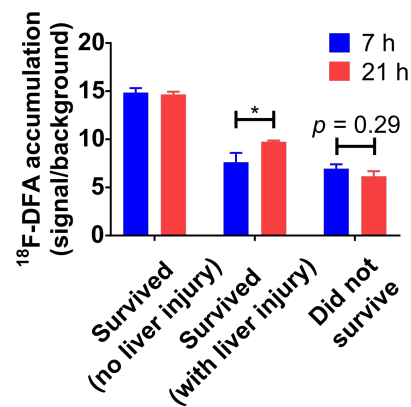


**Figure S6:** A kinetic picture of the liver responding to acetaminophen. Tabulated hepatic  $^{18}\text{F}$ -DFA accumulation, plotted by time point and survival status. Survived (no liver injury), both time points:  $n=8$ ; survived (with liver injury) – 7 h:  $n=2$ ; 21 h:  $n=5$ ; did not survive – 7 h:  $n=6$ ; 21 h:  $n=8$ . Unpaired t tests. \*:  $p<0.05$ .